Supporting information

Identification of the 2-Benzoxazol-2-yl-phenol Scaffold as New Hit for JMJD3 Inhibition

Assunta Giordano,[†,‡] Giovanni Forte,[‡] Stefania Terracciano,[‡] Alessandra Russo,[‡] Marina Sala,[‡] Maria C. Scala,[‡] Catrine Johansson,[§] Udo Oppermann,[§] Raffaele Riccio, [‡] Ines Bruno,[‡] and Simone Di Micco*[,‡]

[†]Institute of Biomolecular Chemistry (ICB), Consiglio Nazionale delle Ricerche (CNR), Via Campi Flegrei 34, I-80078, Pozzuoli, Napoli, Italy.

[‡]Department of Pharmacy, University of Salerno, Via Giovanni Paolo II, 132, 84084, Fisciano, Salerno, Italy.

[§]Botnar Research Centre, Oxford NIHR BRU, Oxford University, Oxford Centre for Translational Myeloma Research, Oxford, OX3 7LD (UK).

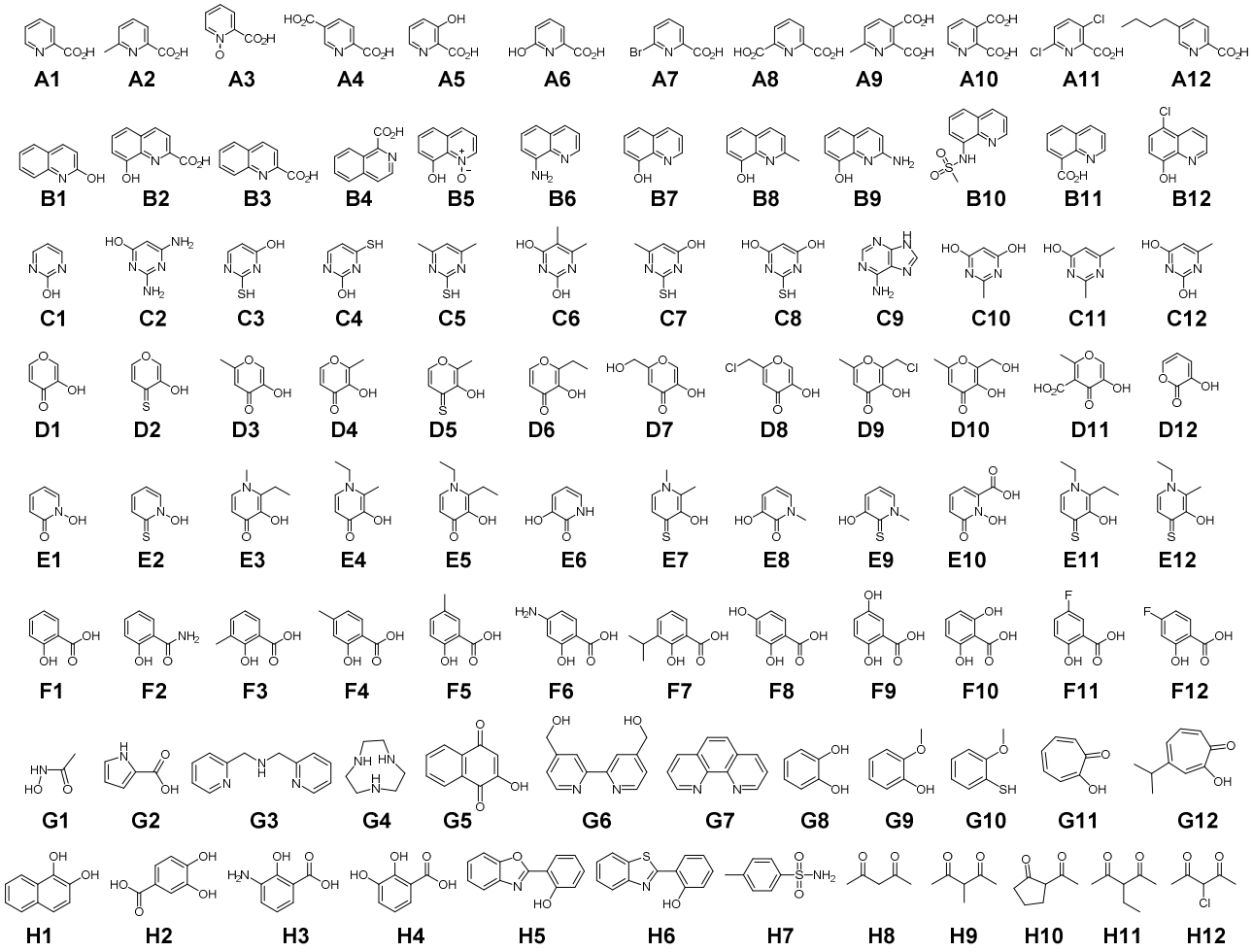

Figure S1. Molecular structures of chelator fragments.

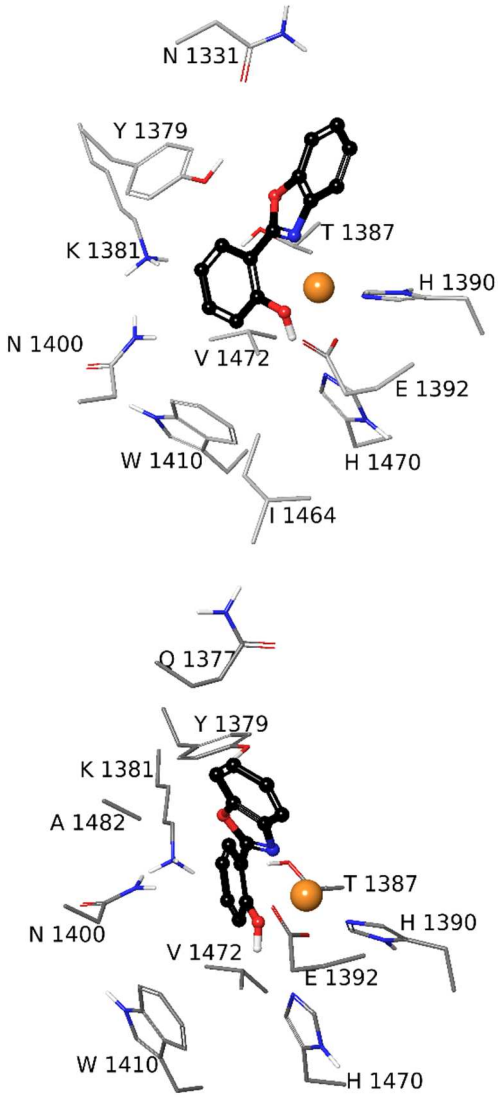

Figure S2. Model A (top, PDB ID: 4ASK) and Model B (bottom, PDB ID: 2XXZ) complexed with H5 (**1**). The fragment is depicted in sticks (black) and balls. Protein residues and $Fe^{2+}$are represented in tube and orange cpk, respectively. The atoms are colored: polar H, white; N, dark-blue; O, red; protein C atom, orange; H5 C atom, black.

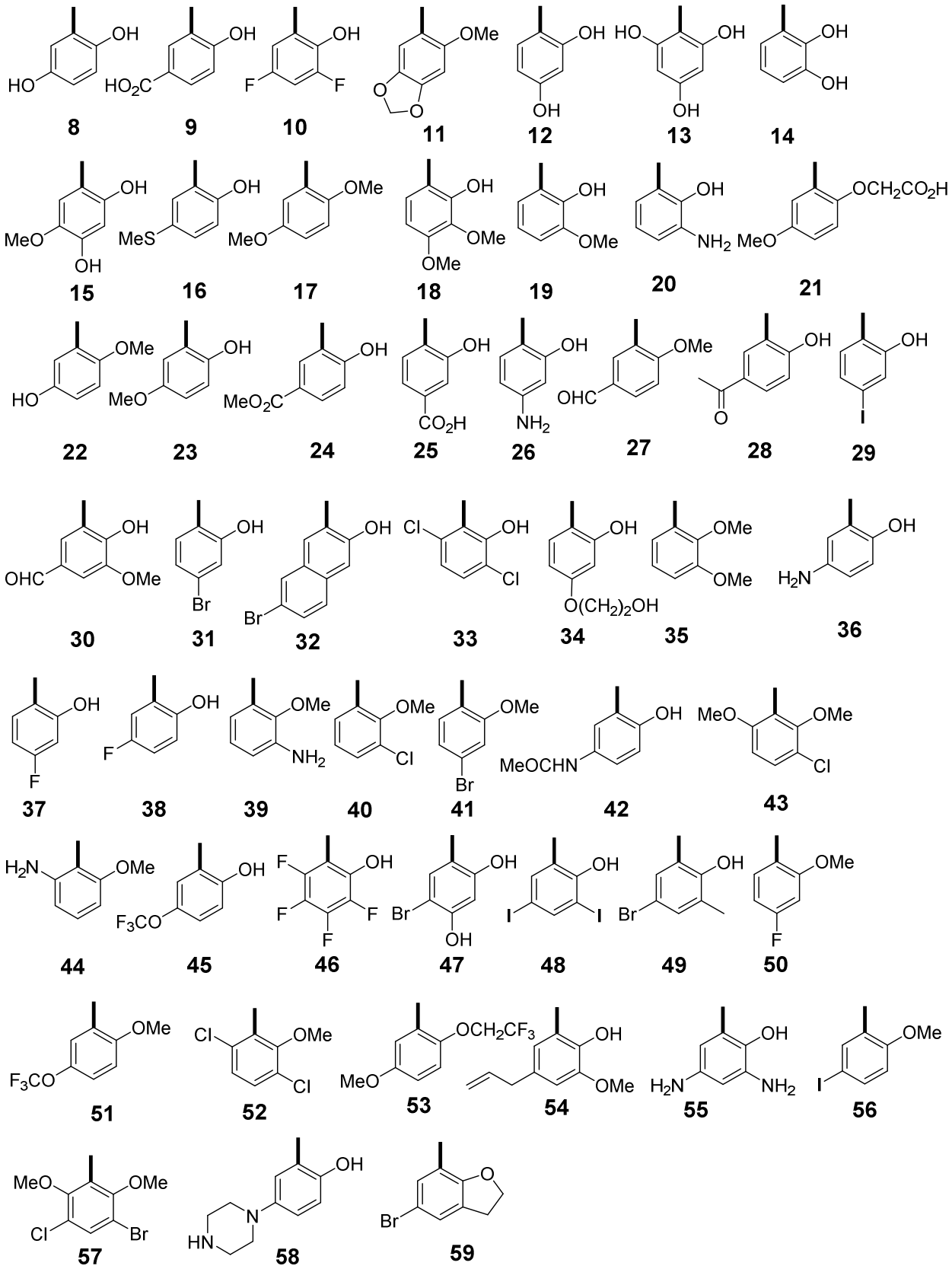

Figure S3. Molecular structures of modified phenol moiety of **1** to obtain compounds **8**-**59**.

Table S1. Free energy of binding and ligand efficiency values calculated by the software Autodock 4.2 for **8**-**59** *vs*. Models A and B.

	Model A		Model B	
compound	Binding energy	ligand efficiency	Binding energy	ligand efficiency
8	-5.69	-0.33	-6.00	-0.35
9	-7.12	-0.37	-9.07	-0.48
10	-4.61	-0.26	-5.71	-0.32
11	-5.27	-0.26	-6.17	-0.31
12	-5.44	-0.32	-5.61	-0.33
13	-5.09	-0.28	-4.37	-0.24
14	-[a]	-[a]	-5.46	-0.32
15	-5.73	-0.30	-5.50	-0.29
16	-5.59	-0.31	-6.64	-0.37
17	-5.43	-0.29	-5.24	-0.28
18	-5.36	-0.27	-5.60	-0.28
19	-5.39	-0.30	-5.22	-0.29
20	-5.27	-0.31	-5.51	-0.32
21	-9.02	-0.41	-8.57	-0.39
22	-5.60	-0.31	-5.23	-0.29
23	-5.98	-0.33	-6.71	-0.37
24	-6.81	-0.34	-8.01	-0.40
25	-[a]	-[a]	-7.22	-0.38
26	-5.00	-0.29	-[a]	-[a]
27	-6.49	-0.34	-5.83	-0.31
28	-6.84	-0.36	-7.95	-0.42
29	-5.99	-0.35	-6.35	-0.37
30	-6.67	-0.33	-7.02	-0.35
31	-6.03	-0.35	-6.10	-0.36
32	-[a]	-[a]	-6.28	-0.30
33	-[a]	-[a]	-[a]	-[a]
34	-4.90	-0.25	-5.99	-0.30
35	-5.67	-0.30	-5.51	-0.29
36	-5.46	-0.32	-5.61	-0.33
37	-4.91	-0.29	-5.82	-0.34
38	-[a]	-[a]	-6.05	-0.36
39	-4.99	-0.28	-4.92	-0.27
40	-5.72	-0.32	-5.68	-0.32
41	-5.32	-0.30	-5.72	-0.32
42	-6.69	-0.33	-5.83	-0.29
43	-5.82	-0.29	-6.21	-0.31
44	-4.88	-0.27	-5.25	-0.29
45	-5.50	-0.26	-6.13	-0.29
46	-[a]	-[a]	-5.45	-0.27
47	-5.48	-0.30	-6.48	-0.36
48	-6.32	-0.35	-6.80	-0.38
49	-6.12	-0.34	-6.61	-0.37
50	-5.34	-0.30	-[a]	-[a]
51	-5.18	-0.24	-5.44	-0.25
52	-5.57	-0.29	-5.84	-0.31
53	-5.62	-0.24	-5.00	-0.22
54	-6.20	-0.30	-5.05	-0.24
55	-5.19	-0.29	-5.14	-0.29
56	-6.21	-0.34	-6.04	-0.34
57	-5.30	-0.25	-5.99	-0.29
58	-[a]	-[a]	-6.10	-2.80
59	-6.19	-0.33	-6.95	-0.37

[a]not defined docked pose.

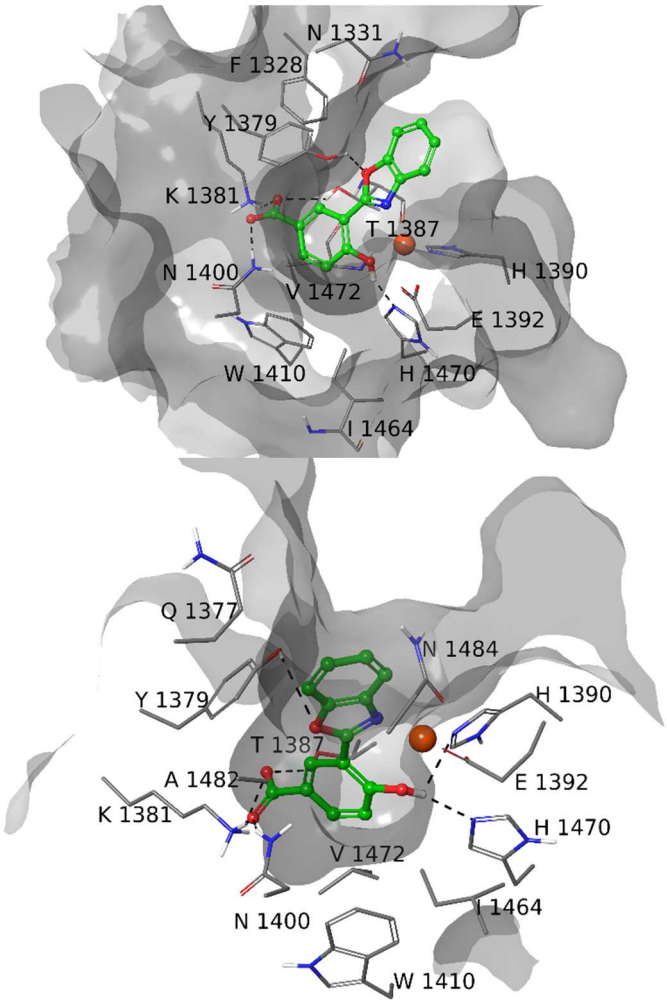

Figure S4. 3D model of the interactions between **9** and the Model A (top) and Model B (bottom) of JMJD3. The protein is represented by molecular surface and tube. **9** is depicted by sticks (green) and balls. The atom color codes are: C (**9**), green; C (JMJD3), gray; polar H, white; N, dark blue; O, red. The dashed black lines indicate the hydrogen bonds between ligand and protein.

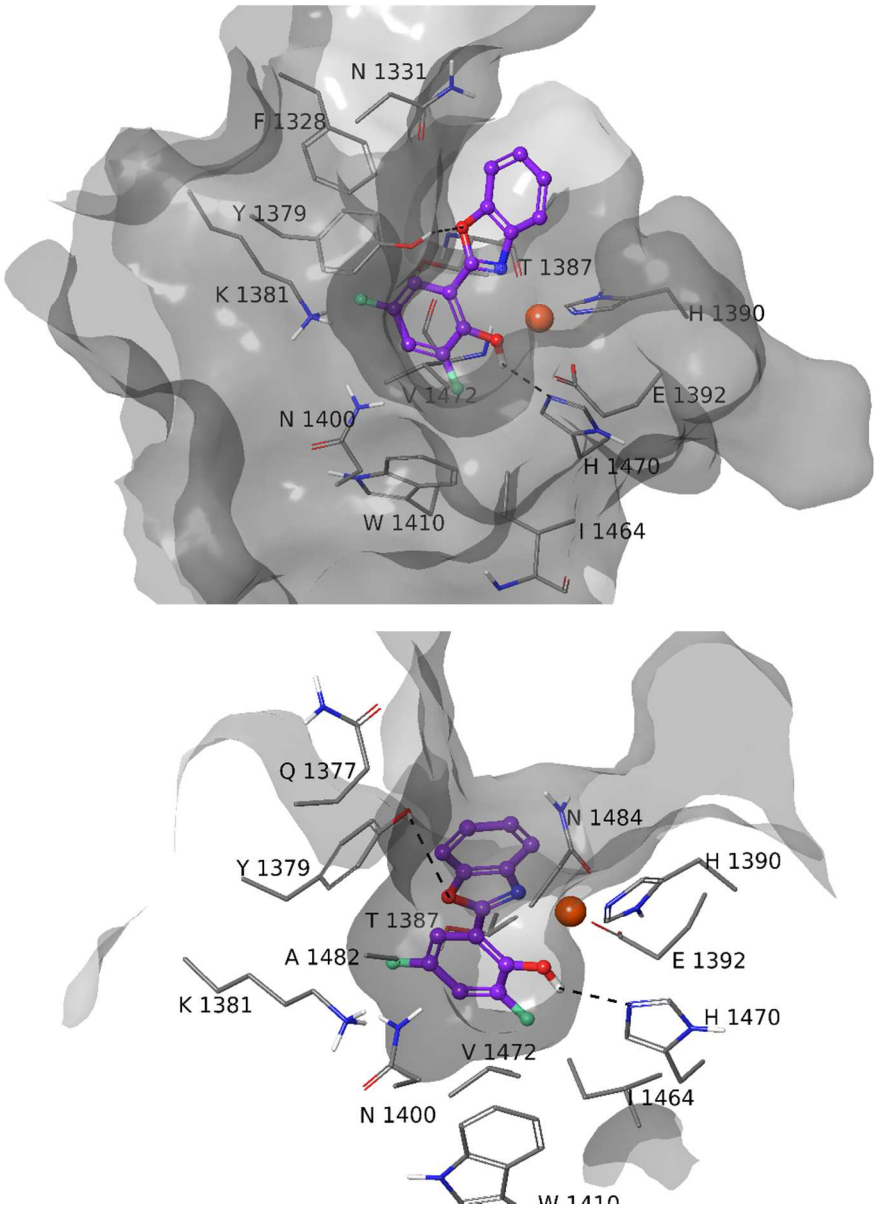

Figure S5. 3D model of the interactions between **10** and the Model A (top) and Model B (bottom) of JMJD3. The protein is represented by molecular surface and tube. **10** is depicted by sticks (purple) and balls. The atom color codes are: C (**10**), purple; C (JMJD3), gray; polar H, white; N, dark blue; O, red. The dashed black lines indicate the hydrogen bonds between ligand and protein.

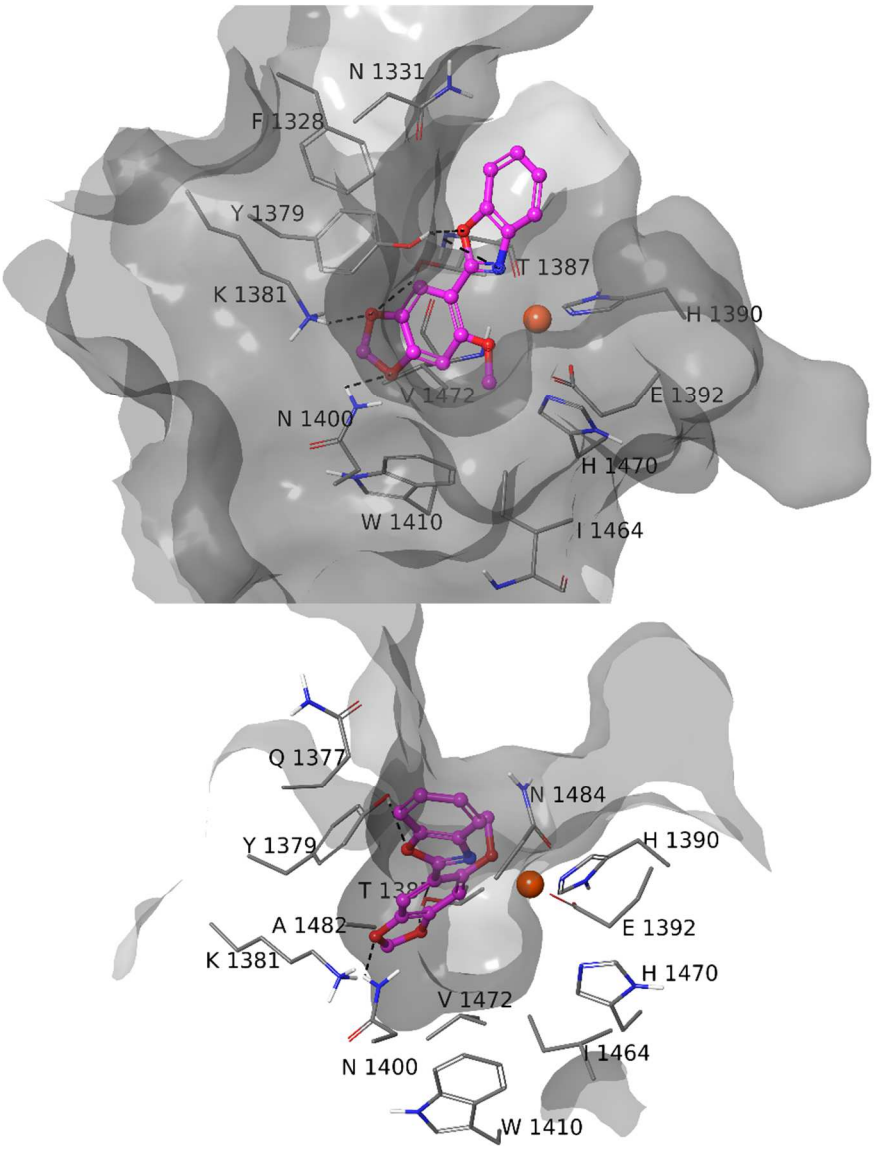

Figure S6. 3D model of the interactions between **11** and the Model A (top) and Model B (bottom) of JMJD3. The protein is represented by molecular surface and tube. **11** is depicted by sticks (pink) and balls. The atom color codes are: C (**11**), pink; C (JMJD3), gray; polar H, white; N, dark blue; O, red. The dashed black lines indicate the hydrogen bonds between ligand and protein.

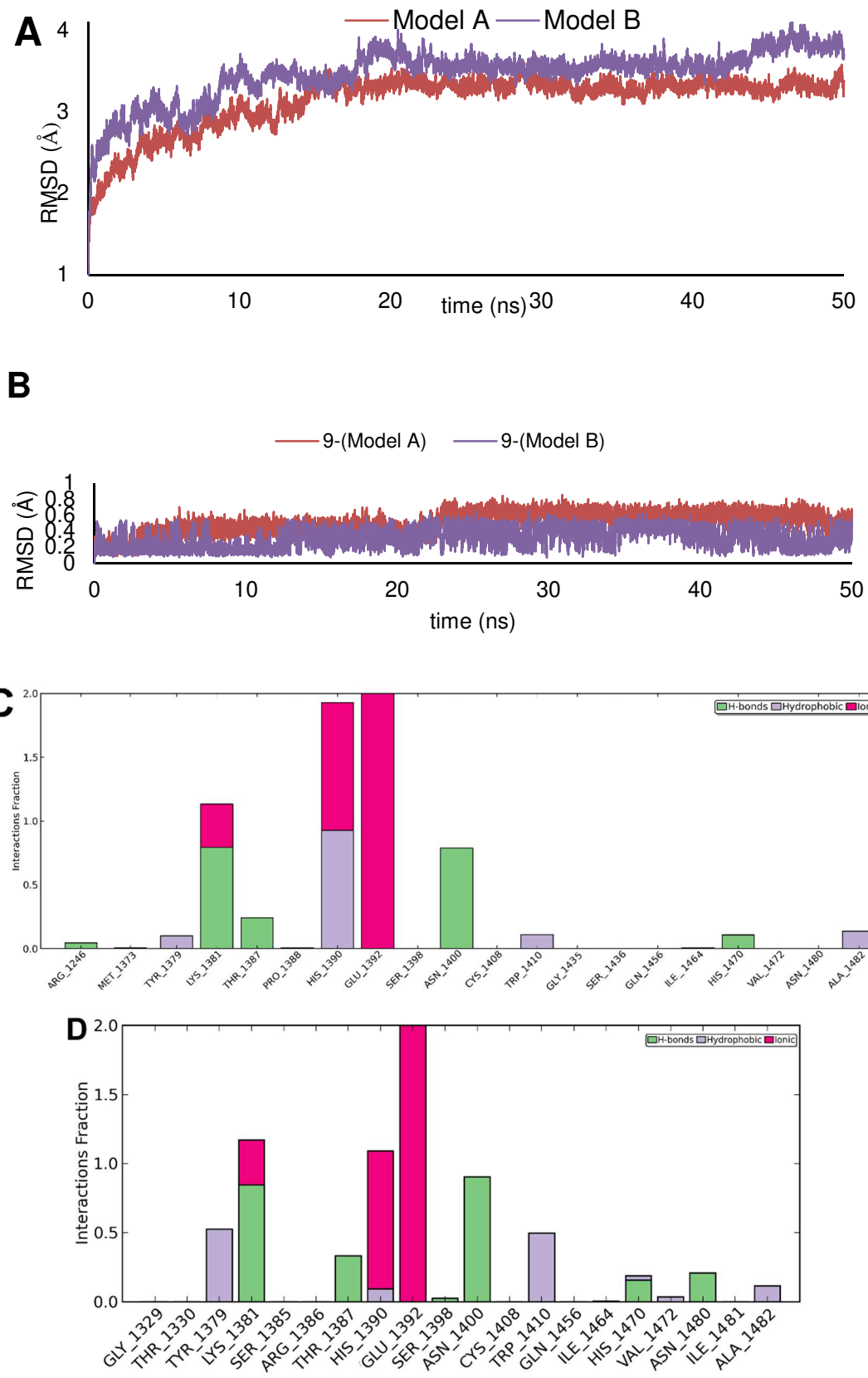

Figure S7. Heavy atom-positional RMSD (Å) as function of simulation time (ns): (A) Models A (brown line) and B (purple line) plot; (B) **9** plot. Protein-ligand contact histograms during the simulation of **9**-Model A (C) and **9**-Model B (D).

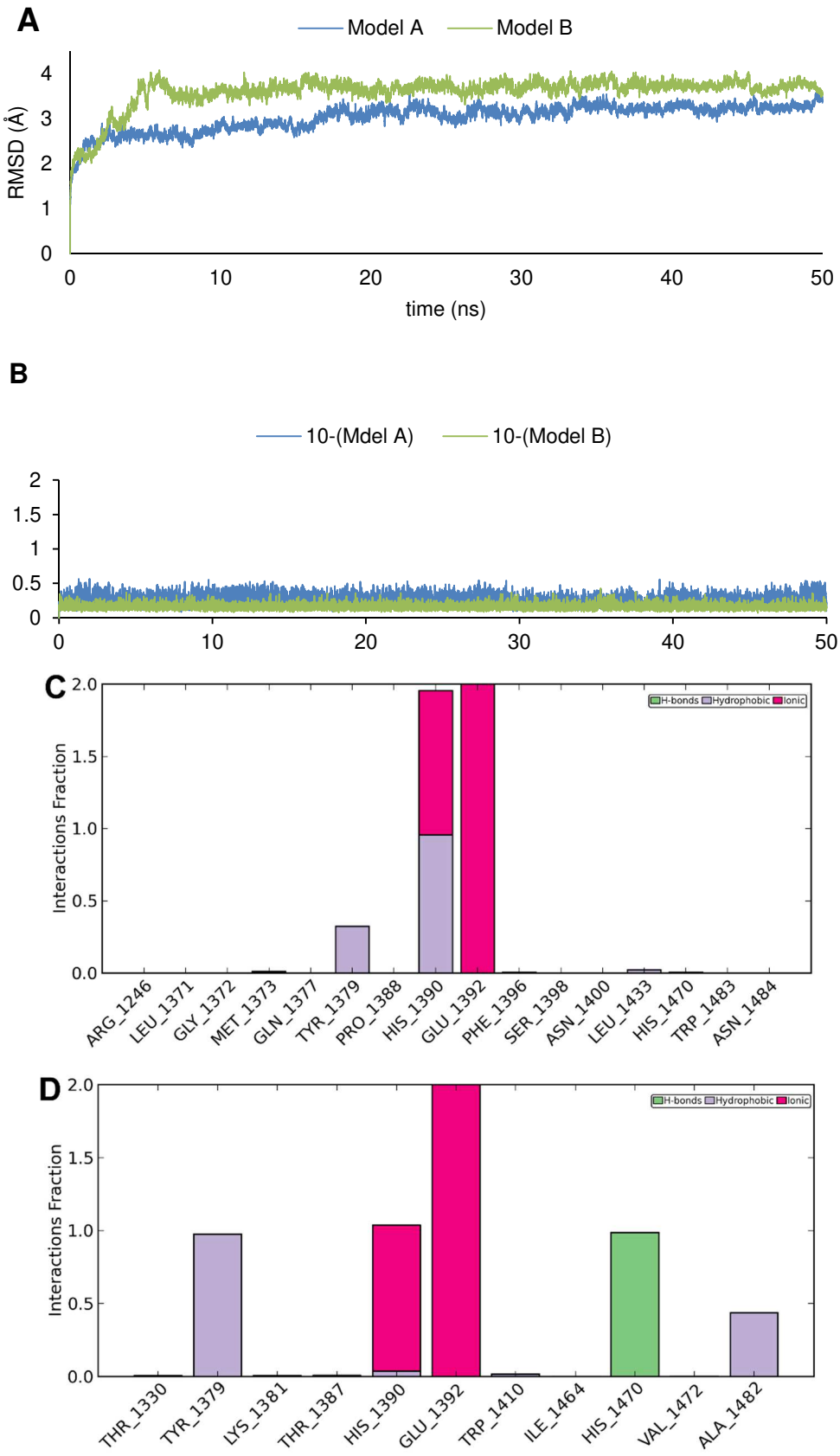

Figure S8. Heavy atom-positional RMSD (Å) as function of simulation time (ns): (A) Models A (blue line) and B (green line) plot; (B) **10** plot. Protein-ligand contact histograms during the simulation of **10**-Model A (C) and **10**-Model B (D).

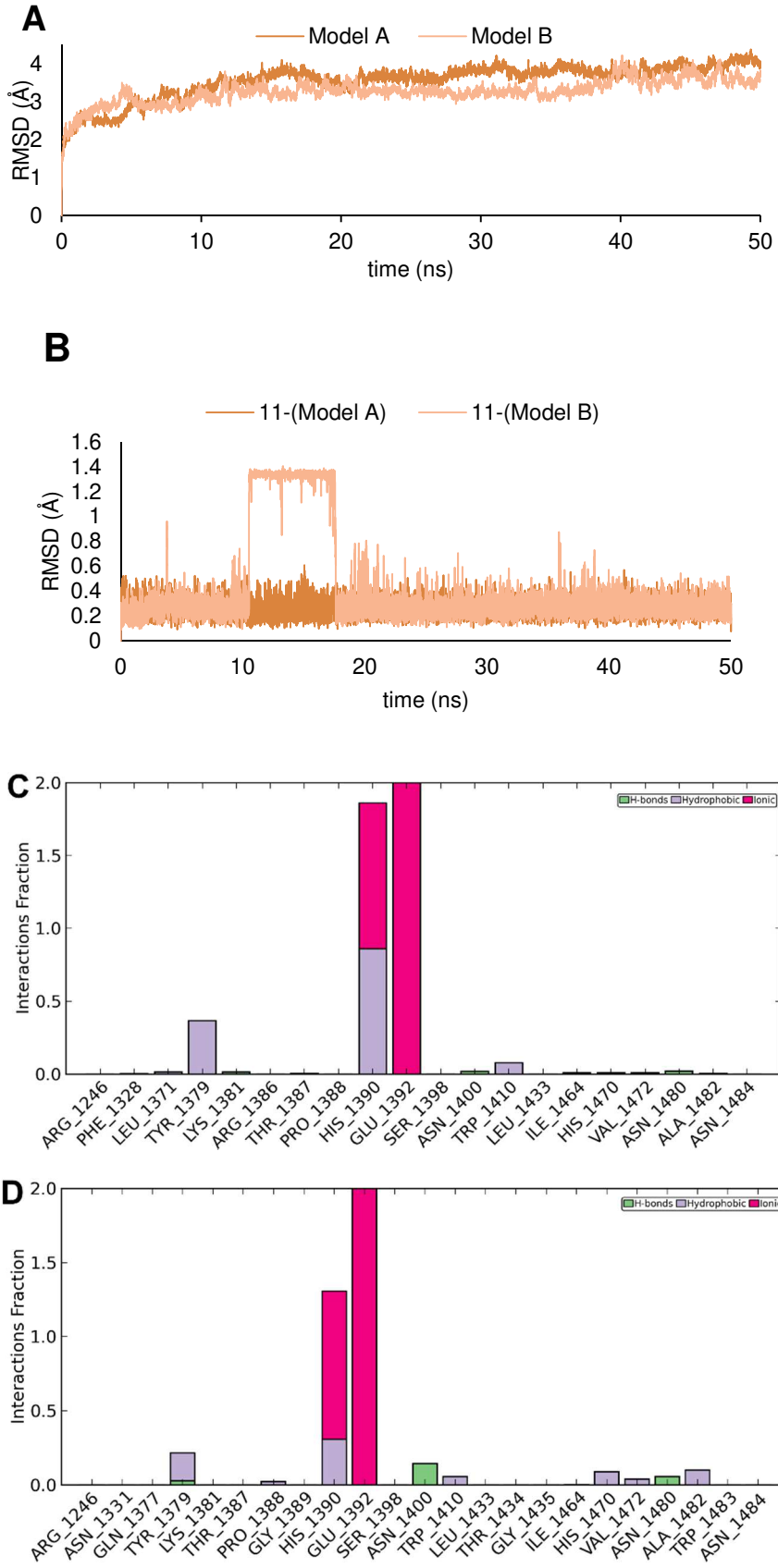

Figure S9. Heavy atom-positional RMSD (Å) as function of simulation time (ns): (A) Models A (light brown line) and B (salmon line) plot; (B) **11** plot. Protein-ligand contact histograms during the simulation of **11**-Model A (C) and **11**-Model B (D).

Table S2. Cell cycle analysis by FACS of A375 treated with **8**. Data are presented as the relative fluorescence intensity of sub-population in percentage of cells in a given sub-population.

Conc. (μM)	G1-Phase (%)	S-Phase (%)	G2/M-Phase (%)
0	59.63	29.56	10.81
20	51.31	47.57	1.12
40	24.14	61.05	14.81
80	21.92	67.12	10.96
100	16.62	73.38	10.00

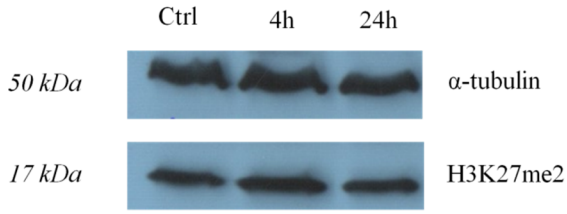

Figure S10. Western Blot assay by an anti-H3K27me2 antibody. The A375 melanoma cell lines were incubated with 100 μM of compound **8** for 4 hours and 24 hours.

Experimental details

Molecular modeling

Maestro version 11[1] was used to build all small molecule structures. All ligand structures (**1**, **2** and **8**-**59**) were optimized through the MacroModel 11.5,[2] using the OPLS3 force field[3] and the Polak-Ribier conjugate gradient algorithm (PRCG, maximum derivative less than 0.001 kcal/mol). All representative conformations for each ligand were refined by using the Polak-Ribier conjugate gradient algorithm (maximum derivative less than 0.001 kcal/mol). To mimic the presence of H_2O, the GB/SA (generalized Born/surface area)[4] solvent treatment was used, in the geometry optimization and in the conformational search calculations. All ligands were processed by LigPrep,[5] generating all possible stereoisomers, tautomers, and protonation states at a pH of 7.0 ± 1.0.

As protein models, we used two crystal structures of JMJD3 (PDB IDs: 4ASK and 2XXZ).[6] The proteins were processed as described in our previous work.[7] Docking calculations were performed by means of the software AutoDock 4.2.[8,9,10] The protein models were processed by AutoDockTools1.5.7rc1:[11] all non-polar hydrogens were merged and Gasteiger charges were added. For Fe^{2+} and of the coordinating amino acids (H1390, E1392 and H1470) we used the calculated DFT partial charges as described in our published manuscript.[7] For Model A, a grid box size of 54 x 46 x 54 was applied, with a grid center having the x, y, and z coordinates: 45.578, 44.880, 7.000. For Model B, the grid box was sized as 48 x 52 x 54, and centred at the following coordinates: 44.299, 44.964, 8.492. The grid points for both boxes were spaced by 0.375 Å. Calculations consisting of 20 runs were performed, by applying the Lamarckian genetic algorithm. An initial population of 150 randomly placed individuals was used. The maximum number of energy evaluations and of generations was set up at 1750000 and 2700, respectively. A mutation rate of 0.02 and a crossover rate of 0.8 were used, and the local search frequency was set up at 0.26. These calculation parameters were validated by docking the co-crystallized GSK-J1 with JMJD3, obtaining an RMSD 0.81 Å for the docked pose respect to the crystallized conformation.[7] Results differing by less than 2.0 Å in positional root-mean-square deviation (rmsd) were clustered together and ranked by free energy of binding.

All bonds were treated as active torsional bonds except the double and ester bonds. Docking results were analysed with Auto-DockTools 1.5.7rc1 and figures obtained by using Maestro 11.

Molecular dynamics simulations

The docked poses of **8**-**11** bound to Models A and B were used as input structures for molecular dynamics simulations. The starting complexes were firstly processed with Protein Preparation Wizard and then were prepared by System Builder[12] in Desmond.[13,14] A cubic box with a 10 Å buffer distance, resulting in a system with approximately atoms 44859 for Model A and 49986 for Model B. The TIP3P[15] water model for solvation and OPLS-2005 force field were used,[16] and Na^+ ions were added for electroneutrality. The so built systems were minimized by LBFGS method, with a maximum number of 2000 iterations and a convergence threshold of 1.0 kcal/mol/Å. Then, the minimized systems were underwent the following relaxation protocol: 1) 1 ns of NVT simulation at 10 K, with small time steps and solute non-hydrogen atoms restrained; 2) 120 ps of NVT simulation using a Berendsen thermostat at 10 K, with fast temperature relaxation constant, a velocity resampling every 1 ps and non-hydrogen solute atoms restrained; 3) 120 ps of NPT simulation using a Berendsen thermostat and a Berendsen barostat at 10 K and a pressure of 1 atm (fast temperature relaxation constant, a slow pressure relaxation constant, velocity resampling every 1 ps, non-hydrogen solute atoms restrained); 4) 120 ps of simulate in the NPT ensemble using a Berendsen thermostat and a Berendsen barostat at 310 K and 1 atm, with a fast temperature relaxation constant, a slow pressure relaxation constant, velocity resampling every 1 ps and non-hydrogen solute atoms restrained; 5) 240 ps of NPT simulation using a Berendsen thermostat and a Berendsen barostat at 310 K and 1 atm, with a fast temperature relaxation constant and a normal pressure relaxation constant. MD simulations

of 50 ns at 310 K were performed, using a recording interval of 1.2 ps and an ensemble class NPT (1.01 bar). A 2.0 fs integration time step was used. Each step of equilibration protocol was checked by Simulation Quality Analysis tool of Desmond, monitoring the total energy, potential energy, temperature, pressure and volume. The exa-coordination of Fe^{2+} was also checked.

Chemistry

General methods

All commercially available starting materials were purchased from Sigma-Aldrich and were used as received. All solvents used for the synthesis were of HPLC grade; they were purchased from Sigma-Aldrich and Carlo Erba. All NMR spectra were recorded on a Bruker Avance 400 MHz instrument. All compounds were dissolved in 0.5 mL of the following solvents: methanol-d_4 (Sigma-Aldrich, 99.8 Atom % D); dimethylsulfoxide-d_6 (Sigma-Aldrich, 99.96 Atom % D). Coupling constants (*J*) are reported in Hertz, and chemical shifts are expressed in parts per million (ppm) on the delta (d) scale relative to CH_3OH (3.31 ppm for ^1H and 49.15 ppm for ^{13}C) or DMSO (2.50 ppm for ^1H and 39.5 ppm for ^{13}C) as internal reference. Multiplicities are reported as follows: s, singlet; d, doublet; t, triplet; m, multiplet; dd, doublet of doublets. ^{13}C NMR spectra were obtained at 100 MHz and referenced to the internal solvent signals. DEPTQ experiments (dept polarization transfer with decoupling during acquisition using shaped pulse for 180 degree pulse on f1channel) were acquired at 100 MHz. High resolution mass spectra were acquired on a LTQ Orbitrap XL™ (Thermo Scientific™) for compounds **8** and **9**, and on a Bruker SolariX XR 7T (Bruker Daltonics, Bremen Germany) for compounds **10** and **11**, in positive or negative mode. Reactions were monitored on silica gel 60 F254 (Merck) plates and visualized and under UV light. Analytical and semi-preparative reversed-phase HPLC was performed on Agilent Technologies 1200 Series HPLC using a Jupiter C18 column (250 x 4.60 mm, 5 m, 300 Å, flow rate = 1 mL/min; 250 x 10.00 mm, 10 m, 300 Å, flow rate = 4 mL/min respectively). The binary solvent system (A/B) was as follows: 0.1% TFA in water (A) and 0.1% TFA in CH_3CN (B); gradient condition: from 5% B to 100% B in 50 min. The absorbance was detected at 220 nm. The purity of all tested compound (>95%) were determined by HPLC analysis. All microwave irradiation experiments were carried out in a CEM-Discover® Focused Microwave Synthesis apparatus, operating with continuous irradiation power from 0 to 300 W utilizing the standard absorbance level of 300 W maximum power. The reactions were carried out in 10 mL sealed microwave glass vials. The temperature was monitored using the CEM-Discover built-in-vertically-focused IR temperature sensor. After the irradiation period, the reaction vessel was cooled rapidly (60-120 s) to ambient temperature by air jet cooling

General procedure for the synthesis of benzoxazoles

A mixture of 2-aminophenol **3** (1 mmol) and phenyl acetic acid (1.3 mmol) was placed in a 10 mL microwave glass vial equipped with a small magnetic stirring bar. The mixture was then stirred under microwave irradiation at 250 °C for 2 min. After completion of the reaction, the vial was cooled to 50 °C by air jet cooling before it was opened. It was then diluted with ethyl acetate (10 mL) and washed with sat. $NaHCO_3$ (2 × 10 mL), brine (10mL), dried (Na_2SO_4), and concentrated under reduced pressure to afford the crude product.

A portion of the crude products was purified by semi-preparative reverse phase HPLC.

*2-Benzooxazol-2-yl-benzene-1,4-diol (**8**)*

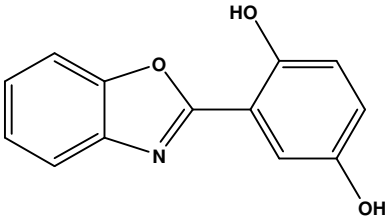

Compound **8** was obtained following the general procedure using 2,5-dihydroxybenzoic acid. RP-HPLC t_R = 30.1 min. Yield 72 %.

^{1}H NMR (CD_3OD, 400 MHz): 7.71 (m, 2H); 7.42 (m, 3H); 6.93 (m, 2H).

^{13}C NMR (CD_3OD, 100 MHz): 164.3; 153.4; 151.5; 150.7; 141.3; 127.0; 126.5; 123.2; 120.2; 119.2; 113.1; 111.9; 111.3.

HR-MS: *m/z* calcd for $C_{13}H_8NO_3$ $[M- H]^-$ 226.0504; found 226.0509.

*3-Benzooxazol-2-yl-4-hydroxy-benzoic acid (**9**)*

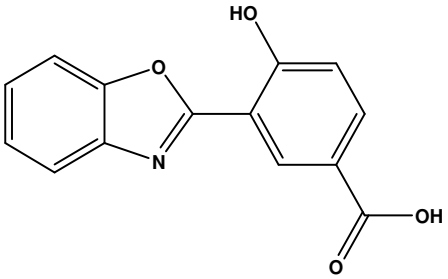

Methyl ester of compound **9** was obtained following the general procedure using 4-hydroxy-isophthalic acid 1-methyl ester. The crude product was subjected to hydrolysis in NaOH 1M for 2 h at 80 °C and then purified by HPLC. RP-HPLC t_R = 28.8 min. Yield 45 %.

^{1}H NMR (CD_3OD, 400 MHz): 8.75 (s, 1H); 8.12 (d, *J* = 8.7 Hz, 1H); 7.78 (m, 2H); 7.47 (m, 2H); 7.17 (d, *J* = 8.6 Hz, 1H).

^{13}C NMR (DMSO-d_6, 125 MHz): 162.33; 149.5; 148.6; 139.3; 134.9; 129.6; 129.2; 126.1; 125.4; 122.6; 119.2; 117.3; 110.8; 110.5.

HR-MS: *m/z* calcd for $C_{14}H_8NO_4$ $[M- H]^-$ 254.0453; found 254.0458.

*2-Benzooxazol-2-yl-4,6-difluoro-phenol (**10**)*

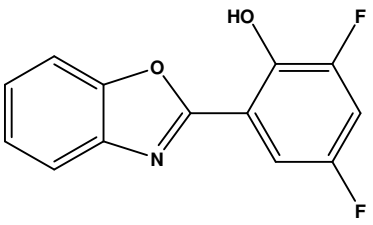

Compound **10** was obtained following the general procedure using 3,5-difluoro-2-hydroxy-benzoic acid. RP-HPLC t_R = 30.5 min. Yield 95 %

^{1}H NMR (CD_3OD, 400 MHz): 7.69 (d, *J* = 8.0 Hz, 1H); 7.46 (m, 2 H); 7.40 (m, 1H); 6.45 (s, 1H); 6.37 (s, 1H).

^{13}C NMR (CD_3OD, 100 MHz): 182.3; 159.5 (d, *J* = 266 Hz); 157.0 (d, *J* = 212 Hz); 152.0; 149.9 (d, *J* = 33.2 Hz); 144.1; 133.7; 130.4; 127.9; 126.7; 117.4; 105.2; 98.8.

HR-MS: *m/z* calcd for $C_{13}H_6F_2NO_2$ [M- H]$^-$ 246.03721; found 246.03752.

*2-(6-Methoxy-benzo[1,3]dioxol-5-yl)-benzooxazole (**11**)*

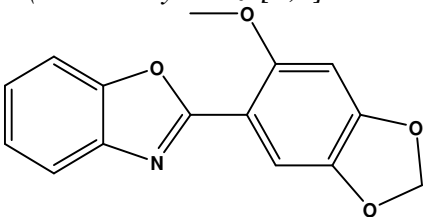

Compound **11** was obtained following the general procedure using 6-methoxy-benzo[1,3]dioxole-5-carboxylic acid. RP-HPLC t_R = 29.1 min. Yield 85 %.

^{1}H NMR (DMSO-d_6, 600 MHz): 7.73 (m, 2H); 7.50 (s, 1H); 7.27 (m, 2H); 7.05 (s, 1H); 6.12 (s, 2H); 3.89 (s, 3H).

^{13}C NMR (DMSO-d_6, 150 MHz): 161.4; 155.3; 151.4; 149.9; 141.3; 141.1; 124.8; 124.4; 119.3; 110.5; 108.7; 107.1; 102.2; 96.0; 57.0.

HR-MS: *m/z* calcd for $C_{15}H_{12}NO_4$ [M+ H]$^+$ 270.07608; found 270.07695.

Alphascreen

Materials

GSK-J1 is purchased from Sigma Aldrich (Italy, Catalog number SML0709).
JMJD3 from Sigma Aldrich (Catalog number SRP0162)
H3K27Me3 Peptide from Anaspec (Catalog number 64367)for JMJD3.
$(NH_4)_2[Fe(SO_4)_2]\cdot 6H_2O$ from Sigma-Aldrich (Catalog number 12304).
L-Ascorbic Acid from Sigma-Aldrich (Catalog number A5960).
2-OG (α-ketoglutaric acid) from Sigma-Aldrich (Catalog number K3752).
Anti-H3K27Me2 from Millipore (Catalog number 07-452).
AlphaScreen General IgG from Perkin Elmer (Catalog number 6760617c)
384-well proxiplates plus from Perkin Elmer (Catalog number 6008280)
AlphaLISA anti-rIgG acceptor beads from PerkinElmer (Santa Clara, CA, Catalog number AL104C).
AlphaScreen Streptavidin-conjugated donor beads from PerkinElmer (Santa Clara, CA, Catalog number 6760002).
Primary antibody 6 from BPS (Catalog number 52140F).
Biotinylated histone H3 peptide substrate from BPS for UTX)

Assay conditions

Donor and acceptor beads and primary antibody were incubated for 1 h.[6] The protein and tested compound were incubated for 15 min at 25 °C. To this solution, 5 µl mixture containing assay buffer, alpha-ketoglutaric acid, FAS, L-Ascorbic Acid, biotinylated histone H3 peptide substrate, wad added, to run the enzymatic reaction at a controlled temperature (25 °C) for 60 minutes. 5 µL of AlphaScreen assay buffer containing EDTA (30 mM) and NaCl (800 mM) to stop the JMJD3 reactions.[6] These 15 µl reactions were carried out in wells of 384-well Optiplate (PerkinElmer). After enzymatic reactions, 5 µl of a solution containing Acceptor and Donor and antibody were added to the reaction mix and incubated for 120 minutes. All steps were carried out in assay buffer (50 mM HEPES pH 7.5, 0.1%

(w/v) BSA and 0.01 % (v/v) Tween-20). $(NH_4)_2[Fe(SO_4)_2]\cdot 6H_2O$ was dissolved fresh each day in 20 mM HCl to a concentration of 400 mM and diluted to 1.0 mM in deionized water. All other components were dissolved fresh each day in deionized water. The serial dilution of the compounds was first performed in 100% DMSO with the highest concentration at 10 mM. A final DMSO concentration of 2%. The percentage of inhibition was determined at 25 μM for each tested compound and 10 μM of protein. IC_{50} value was measured by testing 10 concentrations (3×10^{-5} M to 1×10^{-9} M) of **8**.

For UTX, the enzymatic reactions were conducted at room temperature for 60 minutes in a 10 μl mixture containing assay buffer, histone H3 peptide substrate, demethylase enzyme, and the test compound. The serial dilution of the compounds was first performed in 100% DMSO with the highest concentration at 1 mM. Each intermediate compound dilution (in 100% DMSO) will then get directly diluted 30x fold into assay buffer for 3.3x conc (DMSO). Enzyme only and blank only wells have a final DMSO concentration of 1%. From this intermediate step, 3 μl of compound is added to 4 μl of demethylase enzyme dilution is incubated for 30 minutes at room temperature. After this incubation, 3 μl of peptide substrate is added. The final DMSO concentration is 1%. After enzymatic reactions, 5 μl of anti-Rabbit Acceptor beads (PerkinElmer, diluted 1:500 with 1x detection buffer) and 5 μl of Primary antibody (BPS, diluted 1:200 with 1x detection buffer) were added to the reaction mix. After brief shaking, plate was incubated for 30 minutes. Finally, 10 μl of AlphaScreen Streptavidin-conjugated donor beads (Perkin, diluted 1:125 with 1x detection buffer) were added. In 20-30 minutes, the samples were measured in AlphaScreen microplate reader (EnSpire Alpha 2390 Multilabel Reader, PerkinElmer). These experiments were performed by BSP Bioscience.

Data analysis

Enzyme activity assays were performed at least in duplicates at each concentration. The A-screen intensity data were analyzed and compared. In the absence of the compound, the intensity in each data set was defined as 100% activity. In the absence of enzyme, the intensity in each data set was defined as 0% activity. The values of % activity versus a series of compound concentrations were then plotted using non-linear regression analysis of Sigmoidal dose-response curve generated with the equation $Y=B+(T-B)/1+10^{((LogEC50-X) \times Hill\ Slope)}$, where Y=percent activity, B=minimum percent activity, T=maximum percent activity, X= logarithm of compound and Hill Slope=slope factor or Hill coefficient. The IC_{50} value was determined by the concentration causing a half-maximal percent activity.

Cell culture

Human melanoma cell lines, A375, were grown in DMEM, supplemented with 10% fetal bovine serum (FBS), 100 U/ml penicillin, 100 U/ml streptomycin and 2 mM L-glutamine (Cambrex Biosciences, Microtech, Naples, Italy. A375 were treated with compound **8** at different concentration (1-5-10-20-40-80-100 μM), for 24 hours.

Parallel Artificial Membrane Permeability Assay (PAMPA)

Donor solution (0.5 mM) was prepared diluting the compound stock solution (10 mM, DMSO) by using phosphate buffer (pH 7.4, 0.01 M). Filters were coated with 5 μL of a 1% (w/v) dodecane solution of phosphatidylcholine. Donor solution (150 μL) was added to each well of the filter plate. 300 μL of solution mixture of 5% DMSO in phosphate buffer were added to each well of the acceptor plate. **8**, propanolol, and furosemide were tested in triplicate. The sandwich was incubated for 24 h at room temperature under gentle shaking. After the incubation time, the sandwich plates were separated

and 300 µL of the acceptor plate were transferred to vial and measured by HPLC with UV detector at 220 nm. Reference solutions were prepared diluting the sample stock solutions to the same concentration reached with no membrane barrier. The apparent permeability value P_{app} is determined from the ratio r of the compound absorbance observed in the acceptor chamber divided by the theoretical equilibrium absorbance (determined independently) applying the Faller[17] modification of Sugano[18] equation:

$$Papp = -\frac{V_D V_R}{V_{D+} V_R A t} \times \ln(1 - r)$$

In this equation, V_R is the volume of the acceptor compartment (0.3 cm^3), V_D is the donor volume (0.15 cm^3), A is the accessible filter area (0.24 cm^2), and t is the incubation time in seconds.

Cell cycle analysis

A375 melanoma cells (1 x 10^6 cells/ml in 12-well culture plates) were incubated for 24 h in the presence of compound **8**. The cells were washed with PBS, collected with trypsin, incubated with iced ethanol 70% for 2 hours and then stained with a solution containing 0.1% sodium citrate, 0.1% Triton X-100 and 50 mg/ml propidium iodide at 4 °C for 30 min in the dark. Cellular DNA content was evaluated by flow cytometry (BD FACSCalibur flow cytometer, Becton Dickinson, San Jose, CA, USA) and data from 5000 events per sample were collected. The percentages of the elements in the hypodiploid region were calculated using the CellQuest software and those in G0/G1, S and G2/M phases of the cell cycle were determined using the MODFIT software. Data are presented as the relative fluorescence intensity of sub-population in percentage of cells in a given sub-population

Statistical analysis

Results are expressed as mean ± SEM. Statistical differences were evaluated by means of one-way ANOVA followed by Bonferroni's multiple comparison test and/or Student's t-test. P-values less than 0.05 were considered as significant. Each experiment was performed at least more than three times as stated. Treatments were performed in triplicate in each experiment.

Western blot analysis

Cell extracts were lysed in RIPA buffer (50 mM Tris-HCl, 150 mM NaCl, 1.0% Triton X-100, 0.5% sodium deoxycholate, 0.1% SDS, 1 mM PMSF, protease inhibitor cocktail). 50 µg of proteins were loaded in SDS–polyacrylamide gels under reducing conditions and western blot analysis were performed. Proteins were visualized using the chemioluminescence detection system (Amersham) after incubation with primary antibodies against dimethyl-Histone H3 (Lys 27) (Millipore) and α-tubulin (Sigma-Aldrich). The blots were exposed to Las4000 (GE Healthcare Life Sciences) or to X-ray film (Kodak, Rochester, NY).

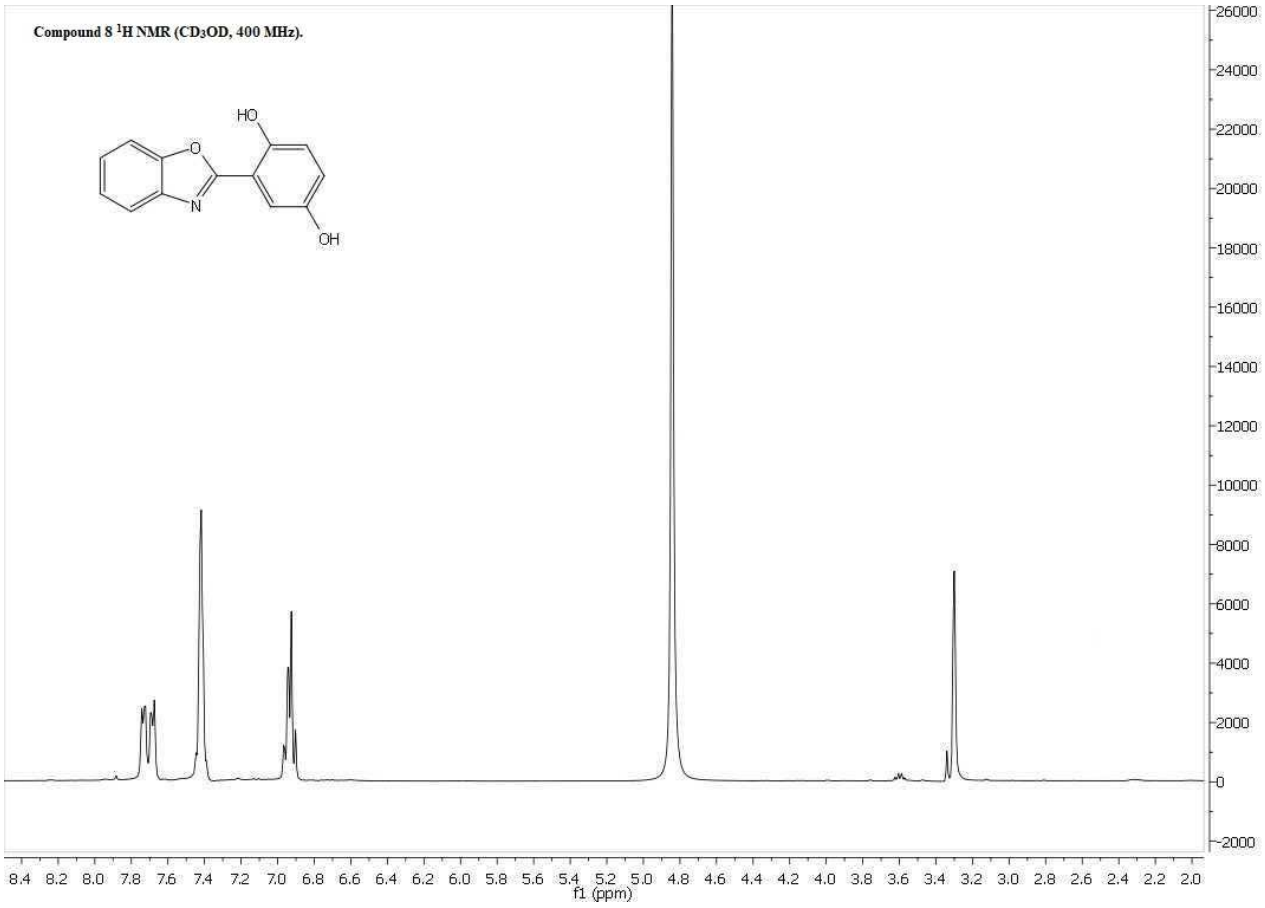
Compound 8 ^{1}H NMR (CD_3OD, 400 MHz).
HO
O
N
OH
26000
24000
22000
20000
18000
16000
14000
12000
10000
8000
6000
4000
2000
0
-2000
8.4 8.2 8.0 7.8 7.6 7.4 7.2 7.0 6.8 6.6 6.4 6.2 6.0 5.8 5.6 5.4 5.2 5.0 4.8 4.6 4.4 4.2 4.0 3.8 3.6 3.4 3.2 3.0 2.8 2.6 2.4 2.2 2.0
f1 (ppm)

Figure S11.

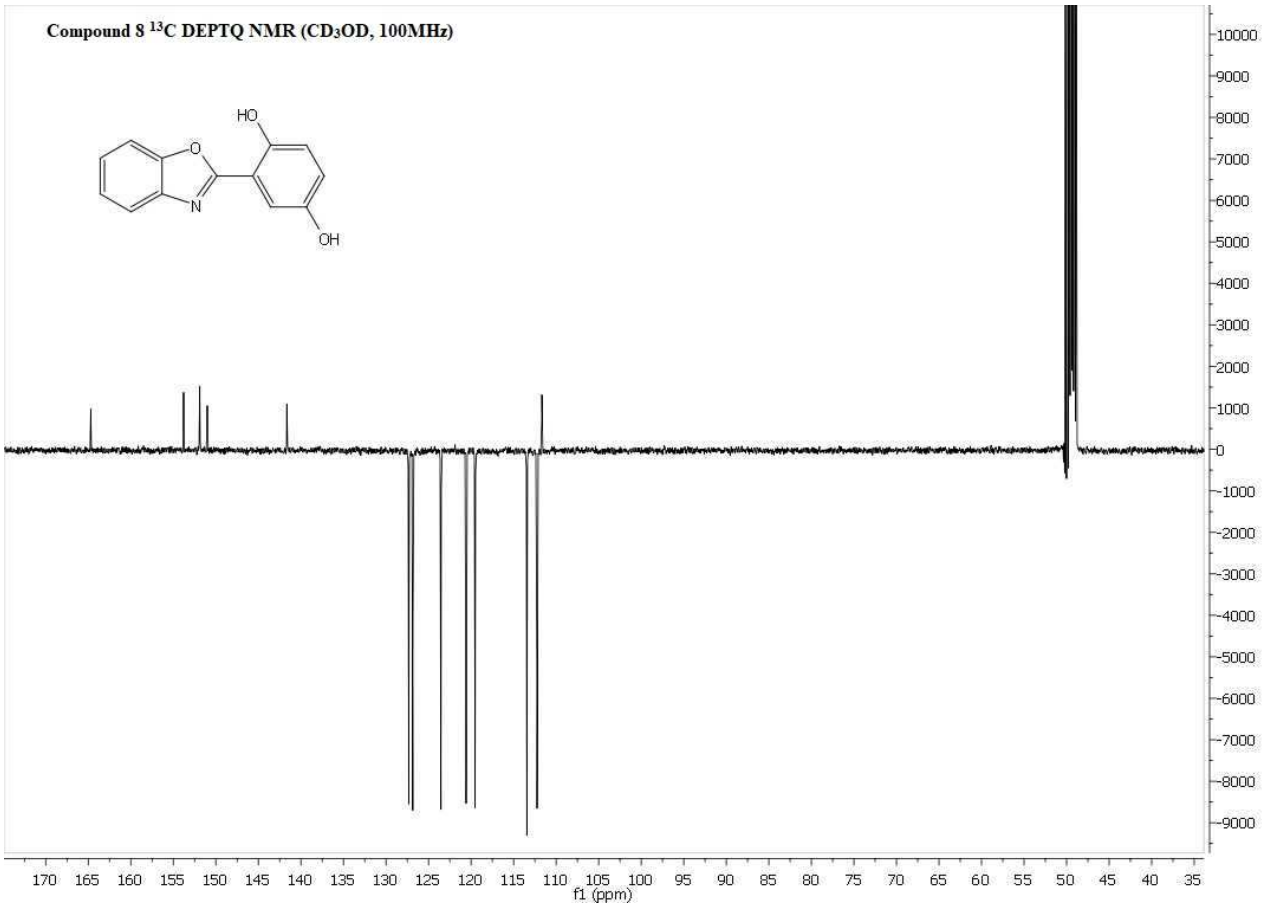
Compound 8 13C DEPTQ NMR (CD3OD, 100MHz)
HO
O
N
OH
10000
9000
8000
7000
6000
5000
4000
3000
2000
1000
0
-1000
-2000
-3000
-4000
-5000
-6000
-7000
-8000
-9000
170 165 160 155 150 145 140 135 130 125 120 115 110 105 100 95 90 85 80 75 70 65 60 55 50 45 40 35
f1 (ppm)

Figure S12.

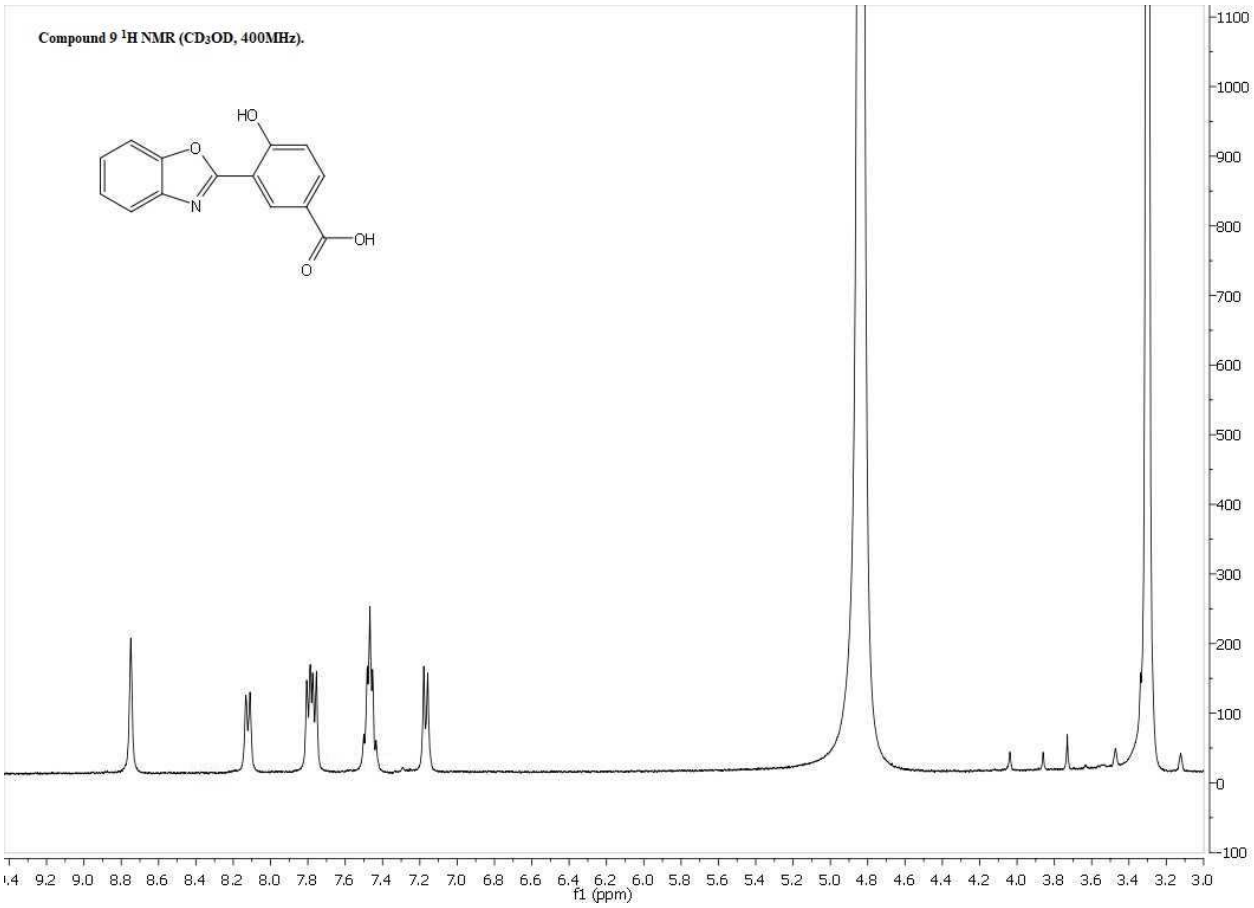

Figure S13.

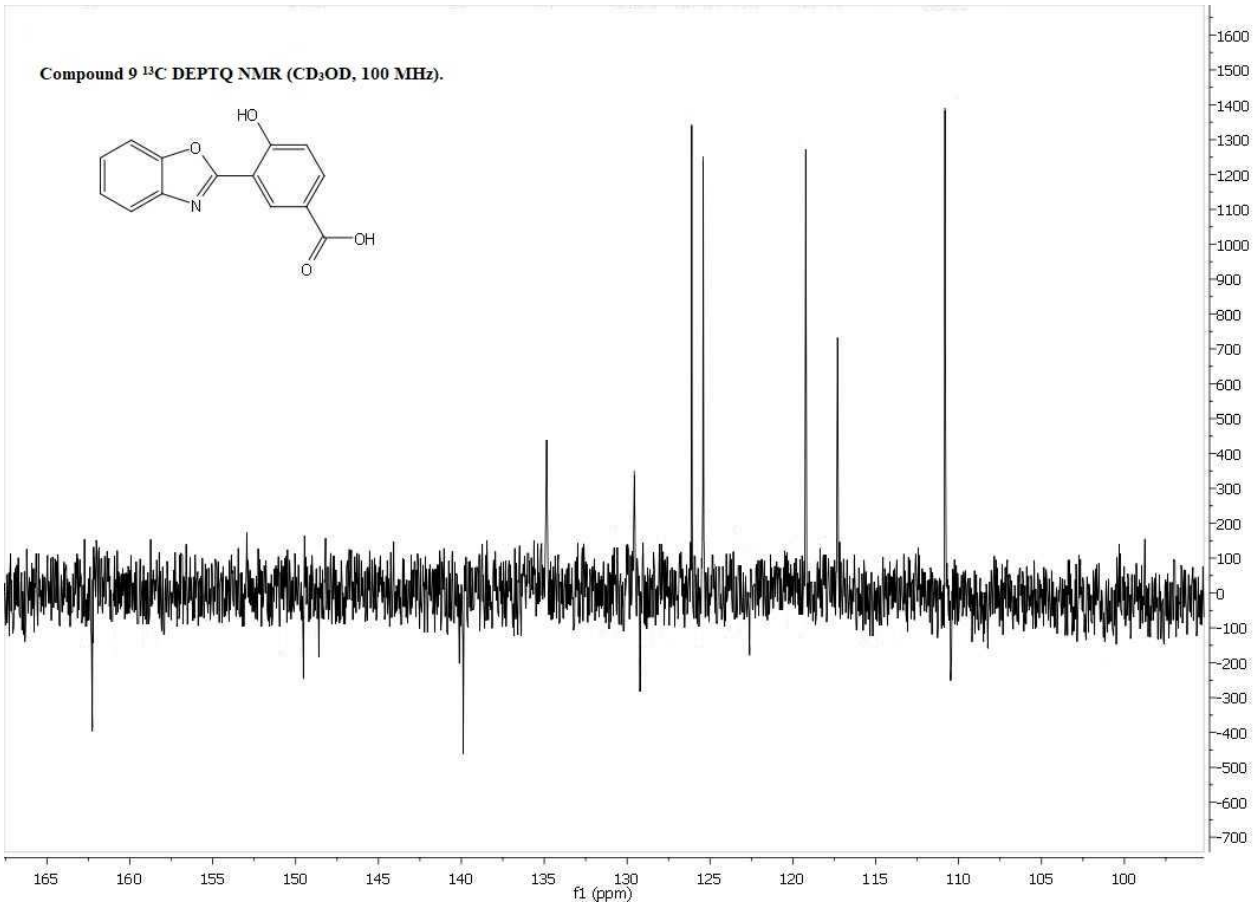
Compound 9 13C DEPTQ NMR (CD3OD, 100 MHz).
HO
O
N
OH
O
1600
1500
1400
1300
1200
1100
1000
900
800
700
600
500
400
300
200
100
0
-100
-200
-300
-400
-500
-600
-700
165
160
155
150
145
140
135
130
125
120
115
110
105
100
f1 (ppm)

Figure S14.

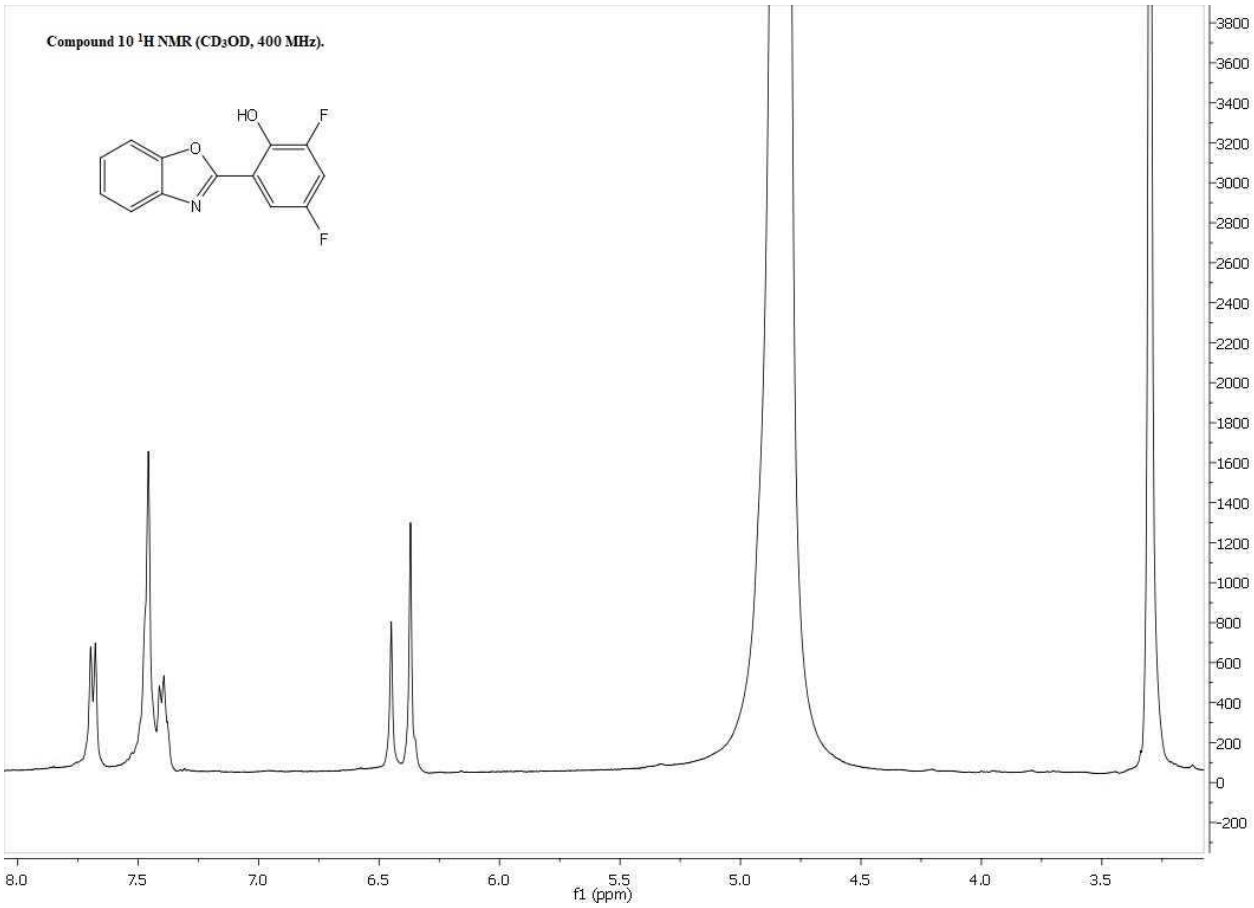
Compound 10 ^{1}H NMR (CD_3OD, 400 MHz).
HO
F
O
N
F
3800
3600
3400
3200
3000
2800
2600
2400
2200
2000
1800
1600
1400
1200
1000
800
600
400
200
0
-200
8.0
7.5
7.0
6.5
6.0
5.5
5.0
4.5
4.0
3.5
f1 (ppm)

Figure S15.

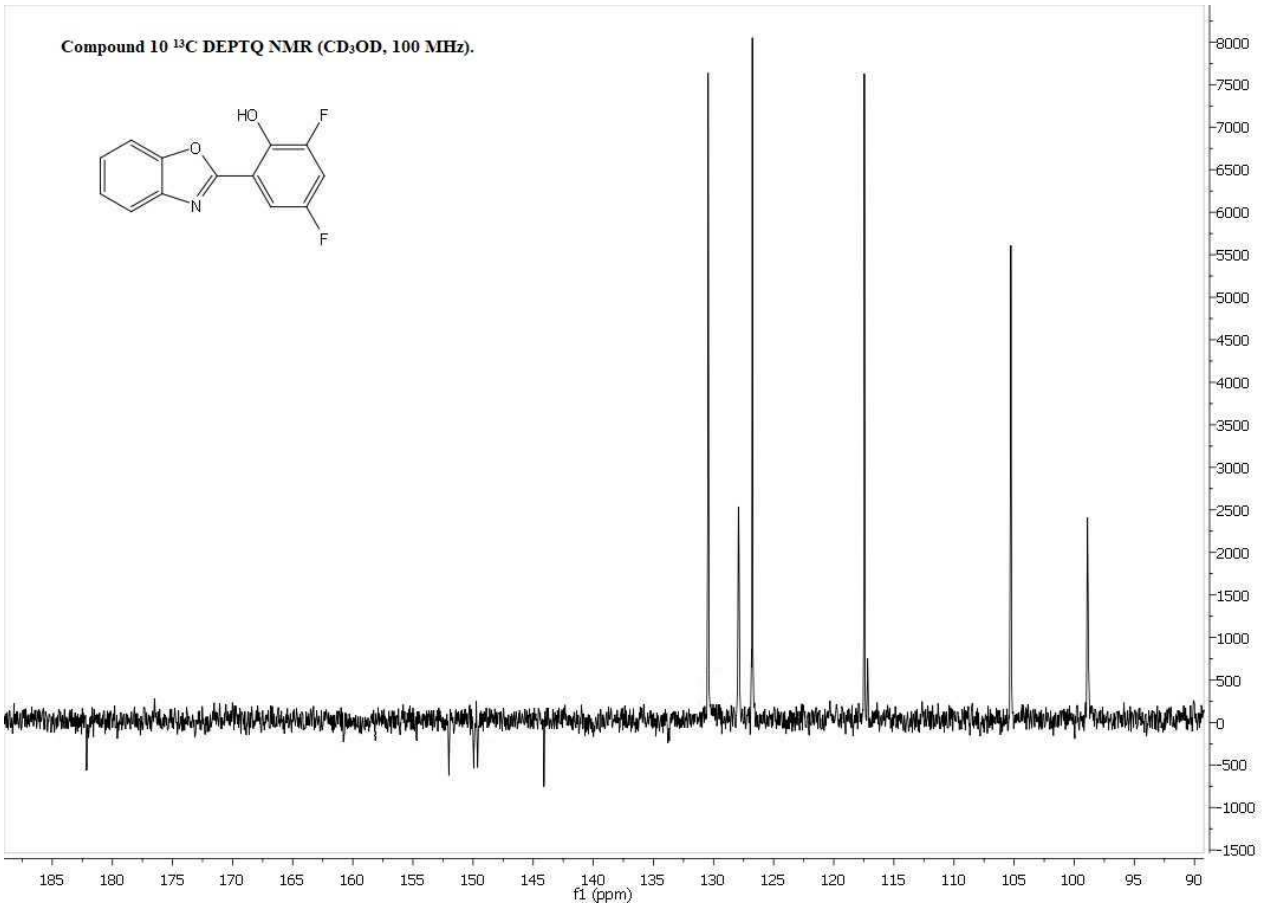
Compound 10 ¹³C DEPTQ NMR (CD₃OD, 100 MHz).
HO
F
O
N
F
8000
7500
7000
6500
6000
5500
5000
4500
4000
3500
3000
2500
2000
1500
1000
500
0
-500
-1000
-1500
185
180
175
170
165
160
155
150
145
140
135
130
125
120
115
110
105
100
95
90
f1 (ppm)

Figure S16.

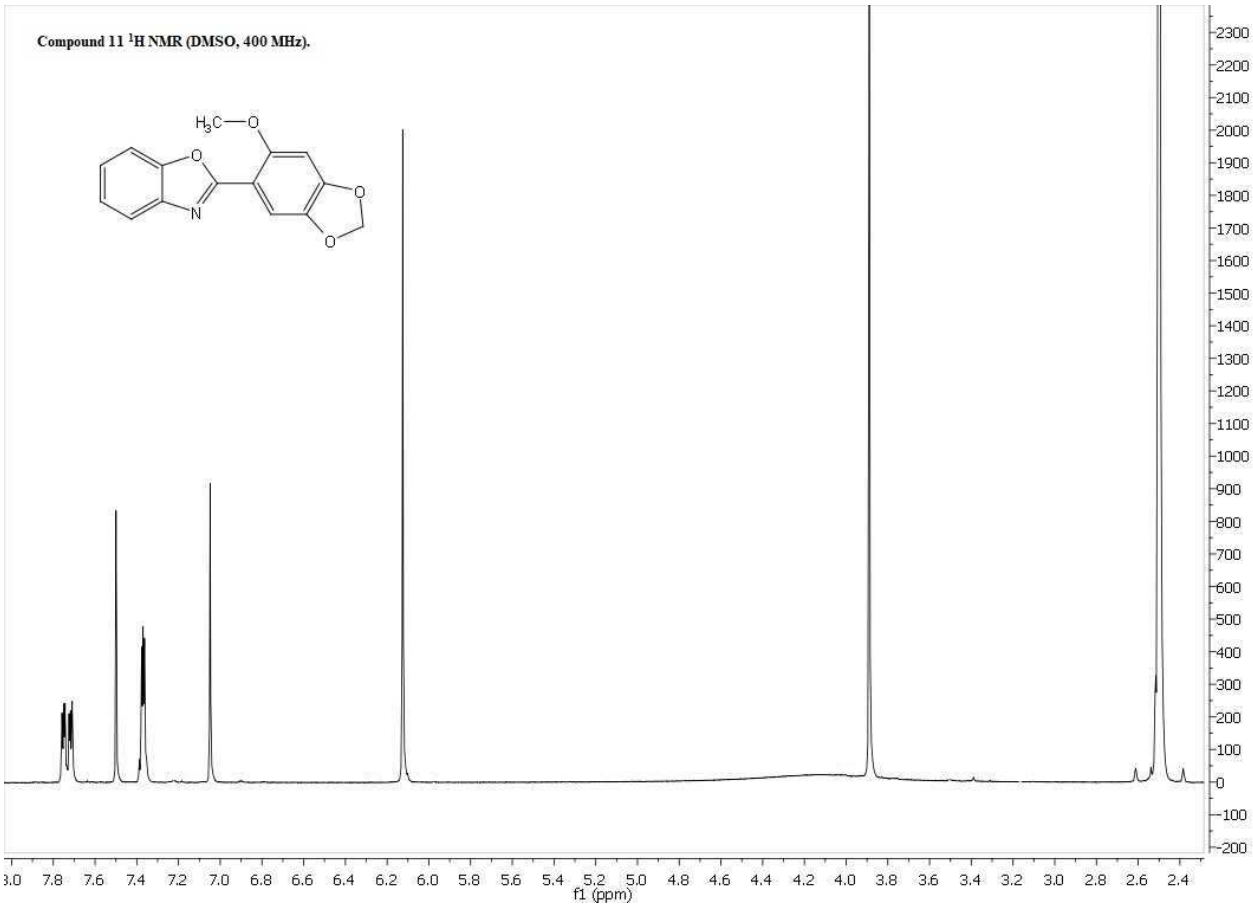

Figure S17.

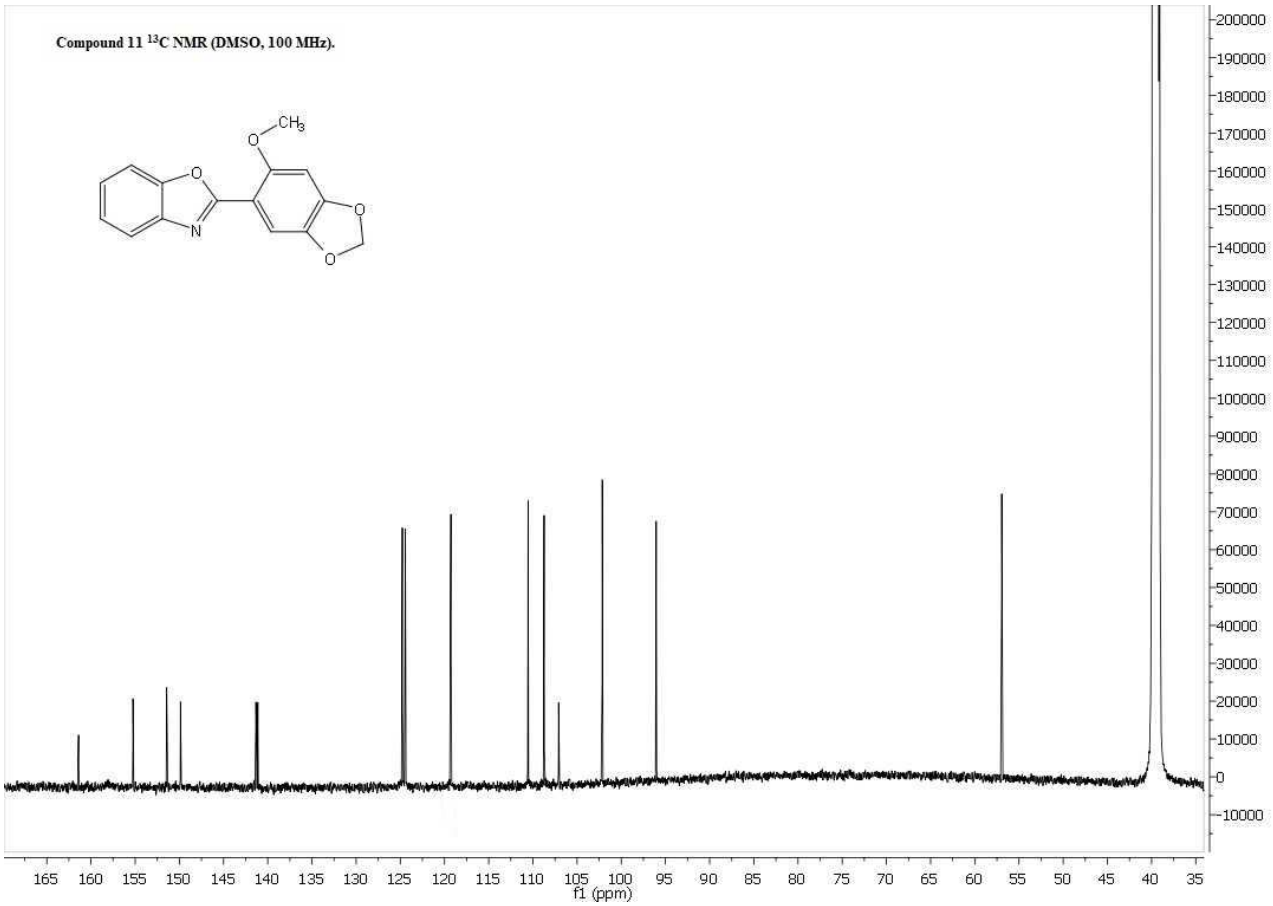
Compound 11 13C NMR (DMSO, 100 MHz).
O
CH3
O
N
O
O
200000
190000
180000
170000
160000
150000
140000
130000
120000
110000
100000
90000
80000
70000
60000
50000
40000
30000
20000
10000
0
-10000
165 160 155 150 145 140 135 130 125 120 115 110 105 100 95 90 85 80 75 70 65 60 55 50 45 40 35
f1 (ppm)

Figure S18.

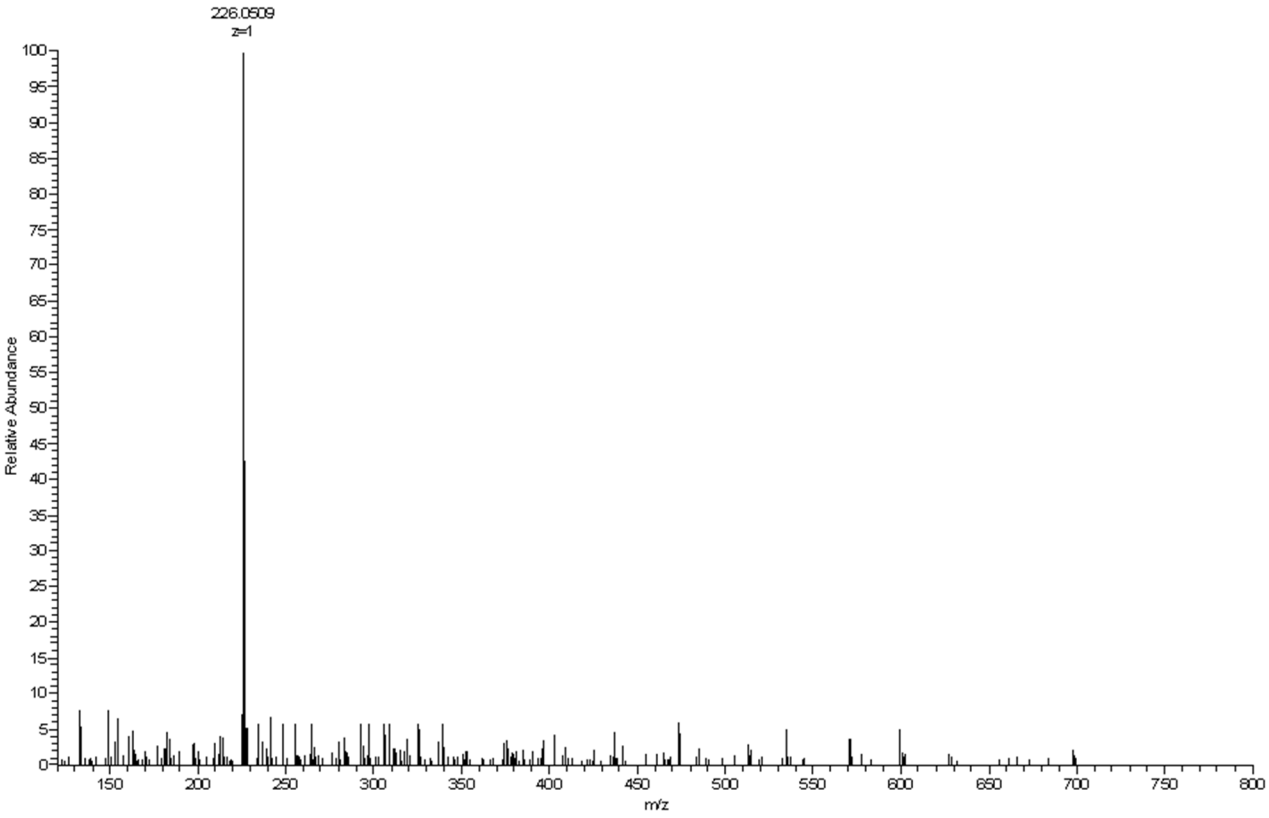

Figure S19. ESI-MS Compound **8**.

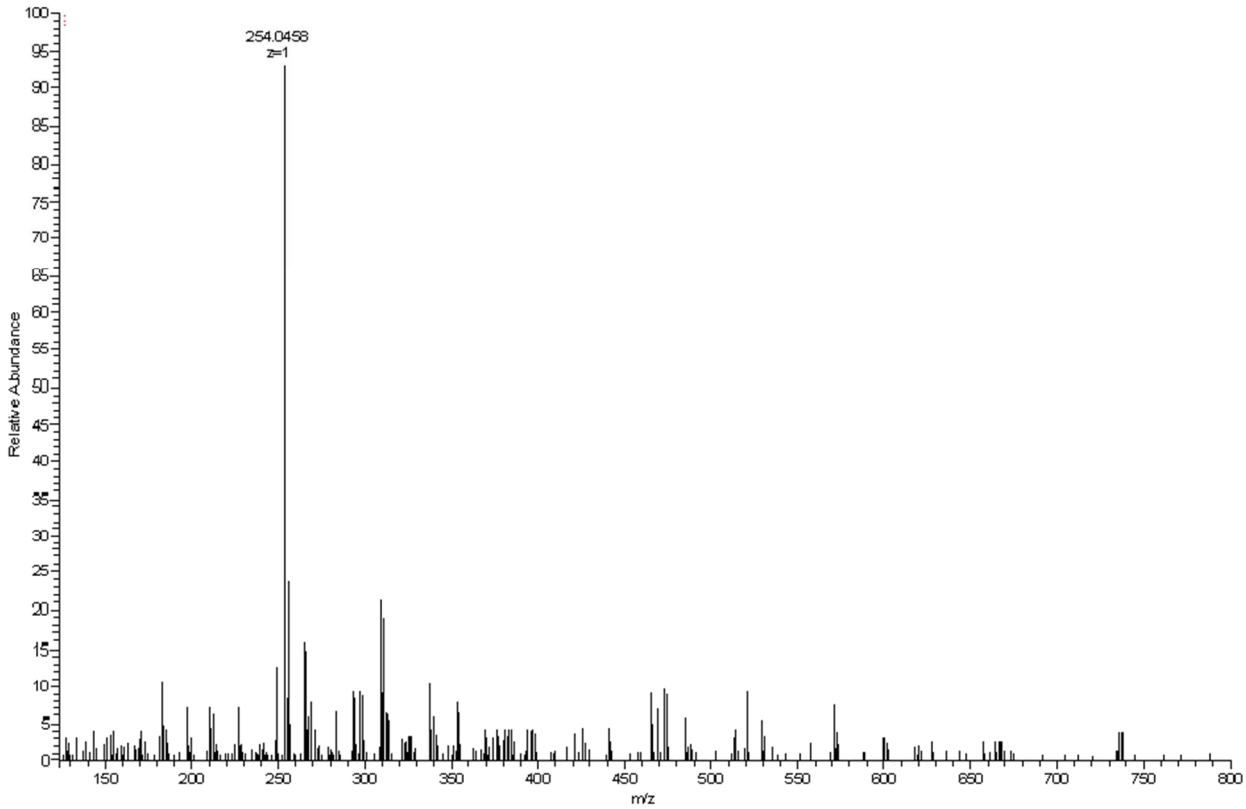

Figure S20. ESI-MS Compound **9**.

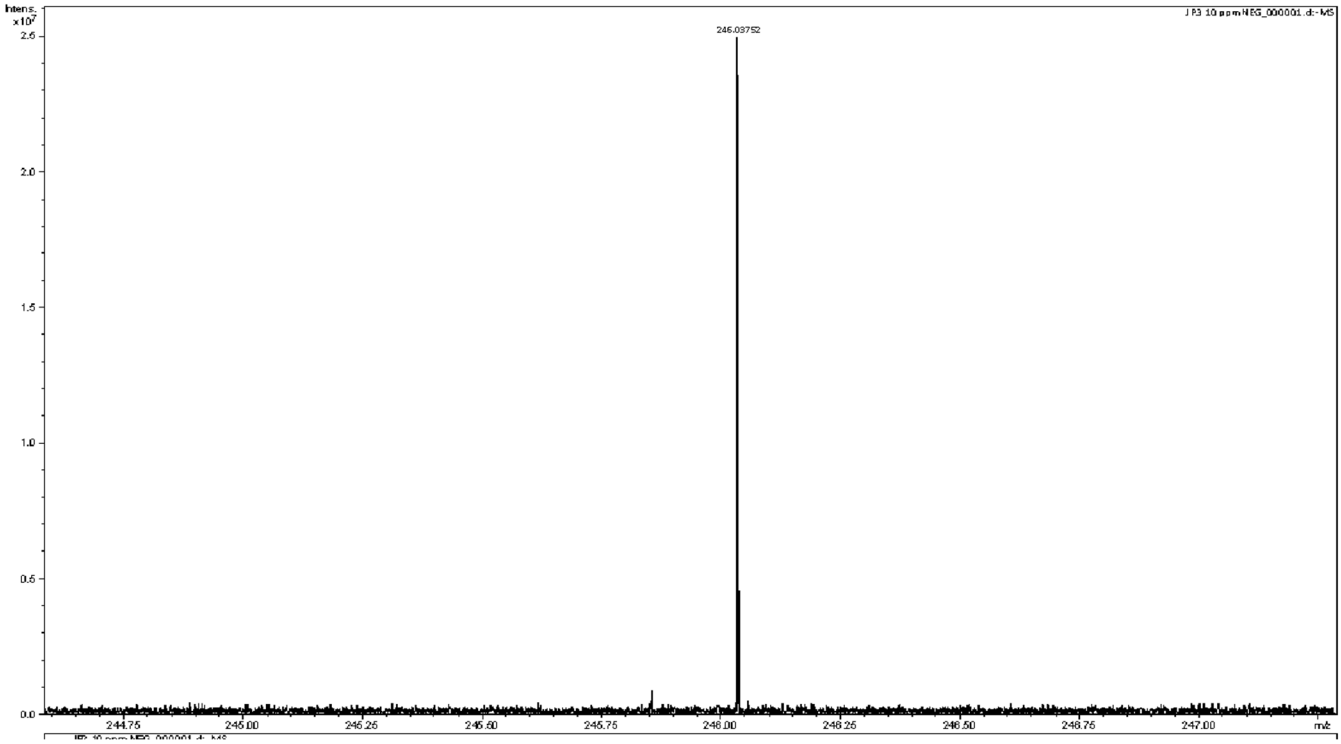

Figure S21. ESI- MS Compound **10**.

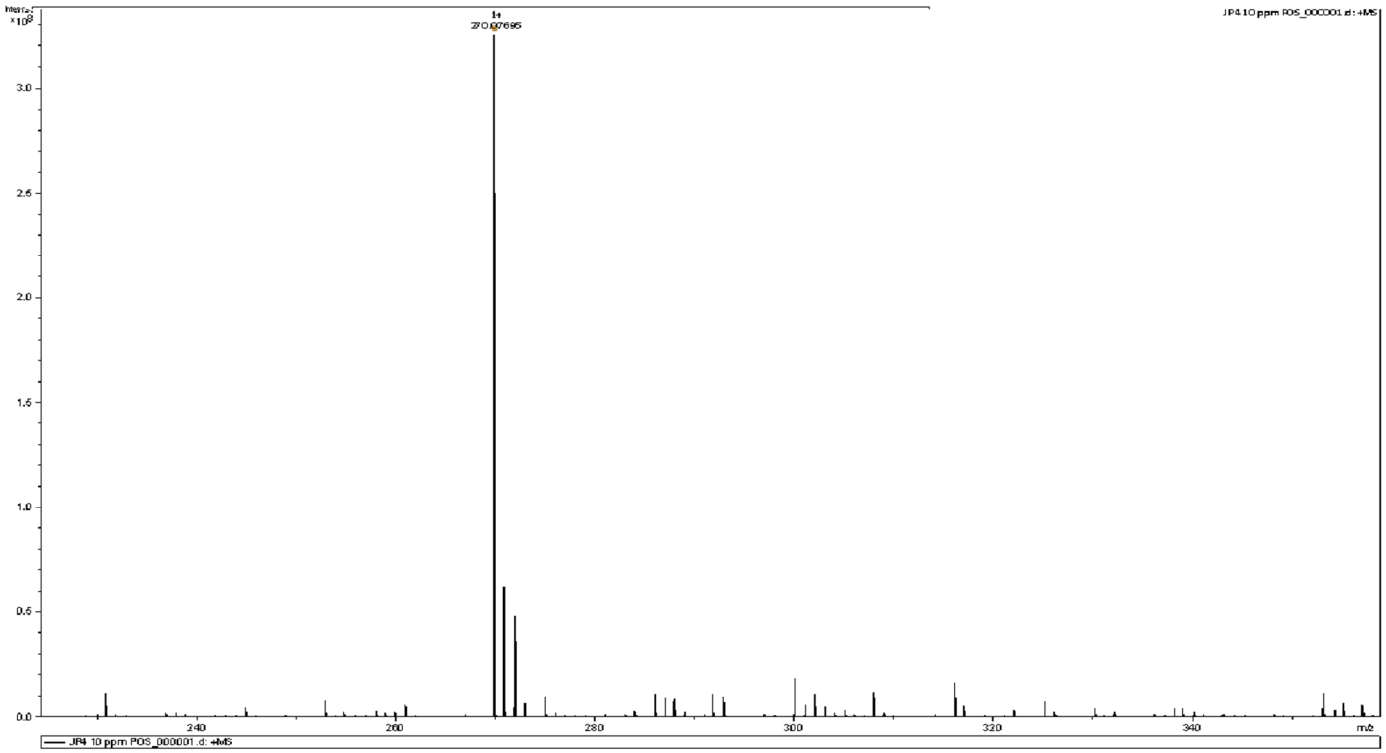

Figure S22. ESI-MS Compound **11**.

References

(1) Schrödinger Release 2017-3: Maestro, Schrödinger, LLC, New York, NY, 2017.
(2) Schrödinger Release 2017-3: MacroModel, Schrödinger, LLC, New York, NY, 2017.
(3) Harder, E.; Damm, W.; Maple, J.; Wu, C.; Reboul, M.; Xiang, J. Y.; Wang, L.; Lupyan, D.; Dahlgren, M. K.; Knight, J. L.; Kaus, J. W.; Cerutti, D.; Krilov, G.; Jorgensen, W. L.; Abel, R.; Friesner, R. A. OPLS3: A Force Field Providing Broad Coverage of Drug-like Small Molecules and Proteins. *J. Chem. Theory Comput.* **2016**, *12*, 281-296.
(4) Still, W. C.; Tempczyk, A.; Hawley, R. C.; Hendrickson, T. Semianalytical treatment of solvation for molecular mechanics and dynamics. *J. Am. Chem. Soc.* **1990**, *112*, 6127-6129.
(5) Schrödinger Release 2017-3: LigPrep, Schrödinger, LLC, New York, NY, 2017.
(6) Kruidenier, L.; Chung, C. W.; Cheng, Z.; Liddle, J.; Che, K.; Joberty, G.; Bantscheff, M.; Bountra, C.; Bridges, A.; Diallo, H.; Eberhard, D.; Hutchinson, S.; Jones, E.; Katso, R.; Leveridge, M.; Mander, P. K.; Mosley, J.; Ramirez-Molina, C.; Rowland, P.; Schofield, C. J.; Sheppard, R. J.; Smith, J. E.; Swales, C.; Tanner, R.; Thomas, P.; Tumber, A.; Drewes, G.; Oppermann, U.; Patel, D. J.; Lee, K.; Wilson, D. M. A selective jumonji H3K27 demethylase inhibitor modulates the proinflammatory macrophager esponse. *Nature* **2012**, *488*, 404 – 408.
(7) Giordano, A.; del Gaudio, F.; Johansson, C.; Riccio, R.; Oppermann, U.; Di Micco, S. Virtual fragment screening identification of a novel Quinoline-5,8-dicarboxylic acid derivative as selective JMJD3 inhibitor. *ChemMedChem* **2018**, *13*, 1160 – 1164.
(8) Morris, G. M.; Huey, R.; Lindstrom, W.; Sanner, M. F.; Belew, R. K.; Goodsell, D. S.; Olson, A. J. AutoDock4 and AutoDockTools4: Automated docking with selective receptor flexibility. *J. Comput. Chem.* **2009**, *30*, 2785-2791.
(9) Cosconati, S.; Forli, S.; Perryman, A. L.; Harris, R.; Goodsell, D. S.; Olson, A. J. Virtual Screening with AutoDock: Theory and Practice. *Expert Opin. Drug Disc.* **2010**, *5*, 597-607.
(10) Forli, S.; Olson, A. J. A force field with discrete displaceable waters and desolvation entropy for hydrated ligand docking. *J. Med. Chem.* **2012**, *55*, 623-638.
(11) Sanner, M. F. Python: a programming language for software integration and development. *J. Mol. Graph. Model.*, 1999, **17**, 57-61.
(12) Maestro-Desmond Interoperability Tools, version 4.2, Schrödinger, New York, NY, 2015
(13) Desmond Molecular Dynamics System, version 4.2, D. E. Shaw Research, New York, NY, **2015**.
(14) Bowers, K. J.; Chow, E.; Xu, H.; Dror, R. O.; Eastwood, M. P.; Gregersen, B. A.; Klepeis, J. L.; Kolossvary, I.; Moraes, M. A.; Sacerdoti, F. D.; Salmon, J. K.; Shan, Y.; Shaw, D. E.; in Proceedings of the 2006 ACM/IEEE Conference on Supercomputing, **2006**.
(15) Jorgensen, W. L.; Chandrasekhar, J.; Madura, J. D.; Impey, R. W.; Klein, M. L. Comparison of simple potential functions for simulating liquid water. *J. Chem. Phys.* **1983**, *79*, 926-935.
(16) Banks, J. L.; Beard, H. S.; Cao, Y.; Cho, A. E.; Damm, W.; Farid, R.; Felts, A. K.; Halgren, T. A.; Mainz, D. T.; Maple, J. R.; Murphy, R.; Philipp, D. M.; Repasky, M. P.; Zhang, L. Y.; Berne, B. J.; Friesner, R. A.; Gallicchio, E.; Levy, R. M. Integrated Modeling Program, Applied Chemical Theory (IMPACT). *J. Comp. Chem.* **2005**, *26*, 1752-1780.
(17) Wohnsland, F.; Faller, B. High-Throughput Permeability pH Profile and High-throughput alkane/water log P with artificial membranes. *J. Med. Chem.* **2001**, *44*, 923−930.
(18) Sugano, K.; Hamada, H.; Machida, M.; Ushio, H. High throughput prediction of oral absorption: improvement of the composition of the lipid solution used in parallel artificial membrane permeation assay. J. Biomol. *Screening* **2001**, *6*, 189−196.